Construction and Building Materials 499 (2025) 144137

Contents lists available at ScienceDirect

Construction and Building Materials

journal homepage: www.elsevier.com/locate/conbuildmat

The use of powdered olive stone in lime-based mortars for the conservation of cultural heritage: A performance evaluation

Maria Antonietta Zicarelli [a], Regina Adomako [b], Silvestro Antonio Ruffolo [a,*], Nicola Schiavon [b], Francesca Giordano [a], Andrea Macchia [c], Mauro Francesco La Russa [a]

[a] Department of Biology, Ecology and Earth Sciences (DiBEST), University of Calabria, 87036 Arcavacata di Rende (CS), Italy
[b] HERCULES Laboratory, University of Évora, Largo Marquês de Marialva 8, Évora 7000-809, Portugal
[c] YOCOCU, Youth in Conservation of Cultural Heritage, Largo dei Quintili 21, Roma 00175, Italy

ARTICLE INFO

Keywords:
Powdered olive stone
Lime-mortars
Conservation
Cultural heritage
Repair mortars
Porosity

ABSTRACT

This research paper investigates the use of Powdered Olive Stone (POS), an agricultural by-product, as a partial replacement for quartz sand in lime-based mortars used for the repair and conservation of historical structures. POS offers a potential solution, addressing waste disposal and reducing reliance on traditional aggregates. This study specifically focuses on lime-based mortars, one of the most commonly used materials in heritage conservation, addressing a research gap regarding the use of POS in this context. In particular, different mortar formulations were prepared by partially replacing natural quartz aggregates with POS at substitution rates of 5 %, 10 %, and 15 %. Additionally, the effect of nano-silica incorporation was evaluated. Following curing, the specimens underwent a comprehensive set of analyses, to examine both mechanical and physical properties of the produced mortars at 28 and 90 days of curing. Such investigations include colorimetric assessment, optical and electron microscopy analyses, capillary water absorption test, ultrasonic pulse velocity measurements, bulk density determination, salt crystallization resistance, and mechanical testing for compressive and flexural strength.

Results: demonstrate that the incorporation of POS resulted in significant modifications of both physical and mechanical properties of the mortars, which can be tailored in order to meet specific requirements of conservation projects.

1. Introduction

The construction industry has a significant impact on environmental dynamics, mostly due to its large-scale use of natural resources [1]. Their long-term exploitation raises serious ecological issues. As the demand for construction materials continues to increase, it becomes crucial for the industry to prioritize sustainable practices and alternative materials to mitigate its environmental impact and preserve natural earth resources for future generations [2]. The increasing demand for sustainable development has spurred a number of scholars to concentrate their research on repurposing discarded or recycled resources as possible building materials. Such approaches include responsible sourcing, recycling building debris, and incorporating alternative materials like agricultural and industrial wastes [3–8].

Utilizing agricultural and industrial by-products in mortar mixes is a type of green construction practice that addresses the issue of waste disposal, while minimizing the use of natural resources such as aggregates in construction and cutting down production cost as well [9].

Studies involving other agricultural by-products like rice husk ash, palm oil clinker, and sawdust as organic aggregates substitute have shown that replacing traditional aggregates with organic materials can reduce the weight of mortar [10–12]. These studies demonstrated that the reduction in density is achievable because the organic materials generally have lower densities than natural mineral aggregates [13].

Among such waste materials, powdered olive stones (POS), have shown potential as an additive or a partial replacement for traditional ingredients in mortar mixtures. A significant amount of solid waste with millions of tons of olive stones produced annually around the world, primarily in Mediterranean regions where olive oil production is concentrated [14], whose disposal causes a major environmental concern. However, it can be used in biofuel production, water treatment and in the construction industry [15]. The adoption of such wastes

* Corresponding author.
E-mail address: silvestro.ruffolo@unical.it (S.A. Ruffolo).

https://doi.org/10.1016/j.conbuildmat.2025.144137
Received 16 July 2025; Received in revised form 4 September 2025; Accepted 19 October 2025
Available online 22 October 2025

would lower buildings' energy consumption, consequently reducing CO_2 emissions and promoting greater energy savings [15].

POS is the solid residue generated after olive oil extraction. It is a lignocellulosic substance with cellulose, hemicelluloses, and lignin as its main component and it offers several benefits, such as affordability and availability, low density, renewable nature, lack of related health risks [16]. The effect of ground olive stones on the mechanical characteristics of mortars has been the subject of a number of investigations. One important finding has been that adding from 20 % to 70 % olive stone usually results in a lower mortar density and improves thermal insulation [17], but potentially compromises its compressive strength. Ferreiro et al. [10], for example, found that the amount of POS used to substitute fine crushed limestone aggregates decreased the mechanical properties of the cement mortar as the proportion of POS increased. Nevertheless, they also pointed out an appropriate application range of 0–30 % where the decrease in the strength of the mortar is not very significant and is acceptable for application [10]. This is also confirmed in a research by Cheboub et al. [18] where it was discovered that replacing natural sand with crushed olive kernel aggregates in a self-compacting lightweight mortar decreased the tensile and compressive strengths, but within the acceptable range limits as stated in the RILEM guidelines for lightweight concrete [19]. Although increasing the amount of POS in a mortar mixture decreases certain properties like workability and setting time, the mechanical strength of the mortar increases with an increase in POS content up to a certain limit as a partial replacement of sand [20].

However, there is a gap in research regarding the use of POS in lime-based mortars. In this research, the POS is used to partially substitute the natural quartz aggregates in varying portions in the preparation of a repair mortar. In particular, lime mortars have been prepared by mixing lime and quartz sand as aggregate, and the latter has been substituted by POS at 5 %, 10 % and 15 %. Moreover, the adding of nanosilica to the mixture has been tested. Several studies have shown that nano-silica can significantly improve the properties of cementitious materials due to its high surface area [21], and reactivity [22], which contribute to a denser microstructure and enhances the interfacial transition zone (ITZ) between the aggregate and the binder, leading to improved bonding [23, 24]. After the setting of the specimens, a series of analyses were conducted, including colorimetric analysis, microscopic and electron microscopic observations, capillary water absorption tests, ultrasound pulse velocity tests, bulk density measurements, salt weathering assessments and mechanical tests to evaluate compressive and flexural resistance.

2. Materials and methods

2.1. Materials and preparation of the specimens

Several lime-based mortars, made by mixing hydrated lime, siliceous sand, Powdered Olive Stone (POS) and eventually nanosilica were prepared.

In particular, three types of mortars were tested:

1. Lime + aggregate + water (reference specimens) (L);
2. Lime + aggregate + powdered olive stone (POSL) in varying proportions (5 % = POS5L; 10 % = POS10L; 15 % = POS15L);
3. Lime + aggregate + powdered olive stone + aqueous suspension of nanosilica (POS-SL) in varying proportions (5 % = POS5-SL; 10 % = POS10-SL; 15 % = POS15-SL).

The binder selected in this study was a hydrated lime (CL70-S) provided by Unicalce S.p.A., from Lecco, Italy. Pure siliceous sand with a particle size distribution between 0.1 and 0.3 mm, supplied by CTS s.r.l., Altavilla Vicentina, Italy, was used as aggregate. POS having grain sizes within 100–315 microns was supplied by BioPowder.com based in Spain. Moreover, the product Nano Estel (CTS s.r.l., Altavilla Vicentina), an aqueous colloidal suspension of silica nanoparticles with an average size of 10–20 nm, with 30 wt% of silica, has been used in the POS-SL specimens' preparation. The nanosilica suspension was first diluted with demineralized water to a concentration of 10 wt% and subsequently allowed to be absorbed by the POS. The diluted nanosilica was added to the POS at a ratio of 0.35 w/w until maximum saturation was achieved, ensuring no excess product was released. Once prepared, the nanosilica-POS mix was added right after to the pastes. For the preparation of all mixtures, deionized water has been used.

Lime/aggregate ratio selected for this study was 1:3 by volume, as it is the most common proportion used in the literature and in conservation practices [25]. POS was added as a partial replacement of sand in different proportions: 5, 10 and 15 % by volume. Moreover, reference mortars (L), exclusively made of lime and sand, were prepared for comparative purpose. A set of three samples per test was produced for each typology.

For each type of mortar mixture, the amount of water to be added was measured by the flow table test [26] to achieve a suitable workability (Table 1). This procedure is repeated three times for each mortar mixture. The degree of spread, or flow, is measured after each trial, and the average spread is calculated to provide a quantitative measure of the mortar's consistency.

All the mortars were manually mixed for 15 min to obtain a uniform paste and then transferred to 50 × 50 × 50 mm cube, 50 x 50 x 20 mm prism and 160 × 40 x 40 mm prism wood moulds in two layers. Each layer was compacted with 10 strokes to remove any air bubbles and voids. The specimens were released from the moulds after 28 days and tested at 28 and 90 days. Samples were cured under controlled environmental conditions (RH 60 ± 10 % and 20 ± 5 °C). Different mortar mixes were prepared according to the proportions presented in Table 1.

2.2. Analytical methodology

All the tests and measurements were performed on the hardened mortars at 28 days, except for the mechanical tests which were conducted on 90 days cured specimens.

2.2.1. Colour measurements

Colorimetric assessment according to EN 15886:2010 [27] has been carried out to evaluate the colour change in the samples with varying concentrations of POS by using a PCE-CSM 7 portable colorimeter. The colour is defined by L^*, a^* and b^* coordinates in the CIE (Commission Internationale d'Eclairage) $L^*a^*b^*$ colour space which represent the lightness, the red/green and the yellow/blue coordinates respectively. Five surface point analyses were selected for each sample, then the average values of the L^*, a^*, and b^* coordinates were then calculated for each mortar typology. The colour coordinates differences (ΔL^*, Δa^* and Δb^*) were obtained by subtracting the L^*, a^*, and b^* values of the olive-stone mortars from the L^*, a^*, and b^* values of the reference ones. Moreover, the total colour differences (ΔE) were calculated according to the Eq. (1).

$$\Delta E = (\Delta L^{*2} + \Delta a^{*2} + \Delta b^{*2})^{1/2} \quad (1)$$

2.2.2. Water absorption by capillarity

To assess the behaviour of the mortars towards water, the determination of the water absorption was investigated according to EN 15801:2010 standard [28]. A filter paper layer of the thickness of about 10 mm was placed on the bottom of a vessel and saturated with distilled water, which amount was kept constant during the entire duration of the test. Then specimens of 50 × 50 x 50 mm dimension were weighted and positioned in contact with the wet layer of filter paper to allow the water absorption by capillarity. The weighting was repeated at time intervals of 10, 20, 30 min and 1, 4, 6, 24, 48, 72, 96, 128, 152 and 176 h until the

Table 1
Mix design of the formulated POS and reference mortars. (v = parts by volume).

Specimens	Lime (v)	Lime (g)	Sand (v)	Sand (g)	Powdered Olive Stone (POS) (v)	Powdered Olive Stone (POS) (g)	Nanosilica/POS ratio (w/w)	Water/Binder ratio (w/w)	Flow (mm)
L	1	85.20	3	718.50	-	-	-	1.75	128
POS5L	1	85.20	2.85	680.96	0.15	13.31	-	2.21	128
POS10L	1	85.20	2.7	645.12	0.3	26.62	-	2.27	128
POS15L	1	85.20	2.55	609.28	0.45	39.94	-	2.30	128
POS5-SL	1	85.20	2.85	680.96	0.15	13.31	0.35	1.88	126
POS10-SL	1	85.20	2.7	645.12	0.3	26.62	0.35	1.88	127
POS15-SL	1	85.20	2.55	609.28	0.45	39.94	0.35	1.88	128

specimens reached the saturated state. The amount of water absorbed by specimens is expressed in function of time as $Q_i = [(m_i - m_0)/A]$ [g/cm^2] where m_i is the mass of the specimen measured at time t_i, m_0 is the mass of the dry specimen and A is the surface area in contact with water.

2.2.3. Salt crystallization test

The durability of the new formulated mixtures against salt decay was evaluated. The prism specimens having dimensions of 50 mm× 50 mm x 20 mm, were subjected to salt crystallization test according to the EN 12370:1999 standard [29] and modified in accordance with the recommendations of [30], [31] and RILEM TC 271-ASC [32], aiming to better simulate real-world conditions. The salt crystallization test was conducted to evaluate the resistance of the specimens to salt-induced weathering, a critical factor in determining the long-term durability of materials used in conservation and restoration. The specimens were initially dried and weighed until a constant mass was achieved. Subsequently, specimens underwent 15 crystallization cycles consisting of 2 h of immersion in a supersaturated solution of sodium sulphate (14 %w/w at 20°C) for 10 % of their height, 8 h of drying in an oven at 45°C and 14 h of cooling at room temperature. The weight of each test sample was measured before the crystallization test and after each cycle and the resulting weight variation (ΔM) was calculated.

2.2.4. Mechanical resistance

The flexural and compressive strength were measured to assess the mechanical performance of the mortars as reported in EN 1015–11:2019 [33]. Flexural strength test was carried out on standard specimens of 160 × 40 x 40 mm to evaluate the mechanical performance of the new formulated mortars. The load was increased uniformly at a rate of 0.2 MPa/s, until failure occurred. The maximum load applied (F) to specimens until failure was recorded and the flexural strength (f_{flex}) was calculated using the Eq. (2).

$$f_{flex} = 1.5\frac{FL}{d^3}\,[MPa] \tag{2}$$

Where L is length of the support span and d is the thickness of the sample. The two halves resulting from the prism specimens were then used for compressive strength measurements. The compressive strength (f_{comp}) was then determined according to Eq. (3):

$$f_{comp} = \frac{F}{d^2}\,[MPa] \tag{3}$$

Where F is the maximum load applied to specimens until failure, and d the thickness of the sample. The resulting flexural and compressive strength values are the mean values calculated for each mortar type.

2.2.5. Ultrasonic pulse velocity test and bulk density measurement

Ultrasonic pulse velocity (UPV) measurements have been performed according to the norm EN 14579:2005 [34]. UPV is an acoustic non-destructive test (NDT) method most often used to evaluate the relative quality, or uniformity, of concrete structures, and to identify the presence of internal flaws such as cracks, voids, and honeycombing. UPV ultrasound speed determination performed by using a Pundit 6 instrument, equipped with two transducers having 54 kHz frequency, employing a solid couplant between the samples and the transducers. Three measurements were conducted for each specimen along the three different axial directions (x, y, z). Then, the ultrasonic pulse velocity was calculated and the average values obtained.

Bulk density values were measured according to the EN 772–13:2002 [35], following the Eq. (4):

$$\rho = \frac{m_{dry}}{V}\left[\frac{g}{cm^3}\right] \tag{4}$$

where ρ is the dry bulk density, m_{dry} is the mass of the specimen after drying to constant mass and V is the apparent volume of the specimen.

2.2.6. Optical microscope and SEM-EDS investigations

Mortar fragments of about 3x3x3 cm of L, POS15 and POS15-S mixtures have been embedded in epoxy resin, then cut and polished on one face to conduct microscopic observations. Optical Microscope (OM) analysis was performed using a Zeiss AxioLab microscope equipped with a digital camera to capture images. Image analysis enabled a quantitative evaluation of the POS particle size distribution within POS15 and POS15-S mortars. In total, nine acquisitions were captured for both the mixtures. Images were first subjected to a standardized post-processing procedure to selectively isolate the olive stone grains from the mortar matrix and then subsequently processed by the software program ImageJ, which is based on Sun-Java and developed by the US National Institutes of Health [36], to calculate the areas of each organic particle. However, when two or more organic particles are in contact or closely packed, the software cannot detect their boundaries as distinct elements and instead interprets them as a single object. As such, larger particle areas may indicate the aggregation of multiple POS grains, reflecting a lack of homogeneous dispersion within the mortar matrix.

In addition, to evaluate whether the olive stone particles in both POS15 and POS15-S mortars belong to the same population, statistical tests, using IBM SPSS software, have been conducted. The Shapiro–Wilk test was performed to evaluate the normality of the POS particles distributions (H_0, null hypothesis = population is normally distributed). Since the data were not normally distributed, the Wilcoxon non-parametric test was carried out to assess the significance of variations among particle distribution (H_0, null hypothesis = particle distributions of each sample come from the same population).

Moreover, Scanning Electron Microscopy (SEM) observations on the polished sections of L, POS15, POS15-S samples have been conducted to characterize the mortar's microstructures. Moreover, the analysis focused on the morphological characterization of olive stone particles and the determination of their chemical composition by means of Energy Dispersive Spectroscopy (EDS). The potential formation of hydraulic phases resulting from the addition of nanosilica in the POS15-S mortars was also evaluated. For these purposes, a Zeiss EVO MA 10 SEM (Carl Zeiss, Oberkochen, Germany) equipped with Thermo NORAN System 7 (Peltier cooled ULTRADRY detector 30mm2) for EDS (Energy Dispersive Spectroscopy) (Thermo Fisher Scientific, Waltham, MA, USA) was used. Spot analyses were performed at 15 kV in a low vacuum mode.

3. Results and discussion

3.1. Colour measurement

Macroscopic observations clearly indicate that the addition of POS to the mixture results in a darker and more yellow appearance of the material (Fig. 1) due to the natural colour of POS particles.

This is confirmed by the colour measurements whose results are summarized in Table 2.

All tested specimens displayed negative ΔL^* values, indicating a progressive shift to darker tones, with the increasing addition of POS content in the mixtures. Indeed, darkening was noted to intensify with higher POS percentages and this trend is evident in both the unmodified and nano silica-modified mortars. In addition, all samples (both POSL and POS-SL mortars) exhibited positive Δa^* and Δb^* values, indicating a shift towards reddish and yellowish hue respectively, moving from 5 % to 15 % of POS replacement.

Nano silica has a lightening effect, helping mitigate the variation to a darker, reddish and yellowish tint at lower POS concentrations, but this effect seems to diminish at higher POS content potentially due to limitations in its ability to counteract the high pigmentation of POS. The total colour difference (ΔE) between POS mortar specimens and reference ones showed significant increases with POS addition, indicating greater visual chromatic deviation. As previously mentioned, although nano silica usually lessened total colour differences, this effect diminished at higher POS levels. The results indicate that the addition of POS yields mortars particularly suitable for applications in which repairs mortars are required to achieve a darker and more yellowish hue. The POS is uniformly dispersed within the mixture, ensuring a homogeneous coloration throughout the material. Nonetheless, it is essential to consider that the colour evaluation for repair mortars should be based on a thorough and preliminary analysis of the original historic surfaces, in order to ensure aesthetic compatibility with the pre-existing materials [37].

3.2. Water absorption by capillarity and durability against salt crystallization

Fig. 2 shows the capillary water absorption curve, illustrating the *Qi* values (water absorbed per unit area g/cm^3) over time for the different mortar specimens. From the data, it can be observed that all specimens show a gradual increase in *Qi* values over time as water absorption continues. The rate of increase is more rapid during the early stages (10–60 min, 25–60 s$^{1/2}$), and it slows down as time progresses (after 6 h, 147 s$^{1/2}$).

L mortars exhibited the highest initial water absorption rate. In contrast, the POS substitution resulted in a slower absorption rate, with increasing of POS content correlating with a progressive decrease of initial water absorption. Concerning the POS-SL mortars, the addition of nanosilica modified the absorption rates compared to the samples containing only POS. As a result, the behaviour of these specimens appears more similar to that of the L mortars.

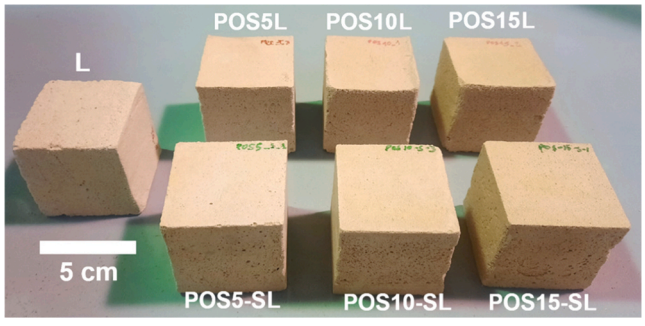

Fig. 1. Macroscopic appearance of the formulated mortars.

After six hours, on the contrary, a significant change in the relative behaviour of the absorption curves was observed. The POSL and POS-SL series closed the initial absorption gap, with specimens containing higher POS content surpassing the L samples in terms of *Qi*. Among these, the POSL series exhibited higher *Qi* values compared to the POS-SL specimens.

This test can provide information on the pore network characteristics of the explored material. In particular, the *Qi* values measured at long terms is proportional to the total open porosity. From the data obtained it can be stated that the inclusion of POS increased the capillarity porosity.

In particular, the higher the percentage of POS, the greater is the porosity of the material. On the other hand, nano silica effectively reduces water absorption by producing a densification of the mortar matrix [38].

Moreover, the overall behaviour of the absorption curves is strongly influenced by the pore size distribution of the mortar systems. The curves corresponding to the POSL and POS-SL mortars exhibit two distinct sections with different slopes, which may be attributed to a bimodal pore size distribution comprising both large and small pores. The larger pores are likely responsible for the rapid water uptake observed at early times, whereas the smaller pores contribute to a slower, sustained absorption phase, as they draw water from the larger pores due to higher capillary pressure [39]. It can be hypothesized that the presence of larger pores arises from the increased water demand associated with the POSL and POS-SL mixtures. Indeed, it is well established that the amount of kneading water significantly affects the pore structure of lime-based mortars, leading to increased overall porosity and a shift toward larger pore diameters as water content increases [40]. This is further supported by the initial hydric behaviour of the POSL mortars, which display a slower absorption rate at higher POS concentrations. This phenomenon is explained by the reduction in capillary sorptivity as pore diameter increases [41]. Conversely, all POS-SL mortars were prepared with a constant water-to-binder ratio, resulting in similar initial absorption rates within this group. Finer porosity, on the other hand, may be introduced through the addition of POS. In this context, when the samples approach saturation, the cavities and voids within the POS could absorb water from the larger pores, which is then gradually diffused into the POS's porous network, resulting in a very slow filling process. Therefore, it can be concluded that both the increased water content and higher POS concentrations contribute to enhanced overall porosity. This increased porosity may, in turn, facilitate greater moisture ingress and the transport of soluble salts, potentially serving a sacrificial function by mitigating further damage to the existing materials [42].

Salt crystallization is widely recognized as one of the main causes of deterioration in porous building materials [43]. The degradation process occurs as a result of repeated crystallization–dissolution cycles within the pore structure, which are strongly influenced by specific thermo-hygrometric conditions [44]. To assess durability against salt crystallization, a reliable accelerated test was conducted under controlled laboratory conditions. The results of this test are presented in Fig. 3, which displays the mass variation curves of the specimens over 15 cycles.

Additionally, photographic documentation of the samples and the associated degradation phenomena observed after each cycle is provided in Fig. 4.

Up to the seventh cycle, all POSL and POS-SL samples experienced an increase in mass due to salt precipitation within the pore structure. Among them, the POS15L specimens showed the most significant gain of 16 %. In contrast, the POS-SL mortar types recorded the lowest mass increases, with POS5-SL reaching only a 9 % increase after the seventh cycle, compared to 13 % in the L mortars.

However, starting from the eighth cycle, the mass variation curve begins to decline toward a point where the gain from salt absorption is

Table 2
Colorimetric coordinates, standard deviation and differences values (ΔL^*, Δa^*, Δb^* and ΔE) between reference mortars and the ones with the POS addition.

	Coordinates			*St. Dev.*			*Variations*			
Specimen	L^*	a^*	b^*	L^*	a^*	b^*	ΔE	ΔL^*	Δa^*	Δb^*
L	88.54	0.64	2.48	0.56	0.12	0.26	-	-	-	-
POS5L	86.39	1.39	5.95	0.70	0.22	0.29	8.63	−2.15	0.75	3.47
POS10L	84.47	2.05	7.78	1.21	0.24	0.37	23.34	−4.08	1.41	5.30
POS15L	84.18	2.32	8.70	0.91	0.22	0.37	30.32	−4.37	1.69	6.22
POS5-SL	86.98	1.18	4.93	1.29	0.27	0.37	4.37	−1.57	0.55	2.45
POS10-SL	84.18	2.24	6.93	0.52	0.19	0.30	20.74	−4.37	1.60	4.46
POS15-SL	83.34	2.66	8.01	0.35	0.15	0.33	30.87	−5.20	2.02	5.53

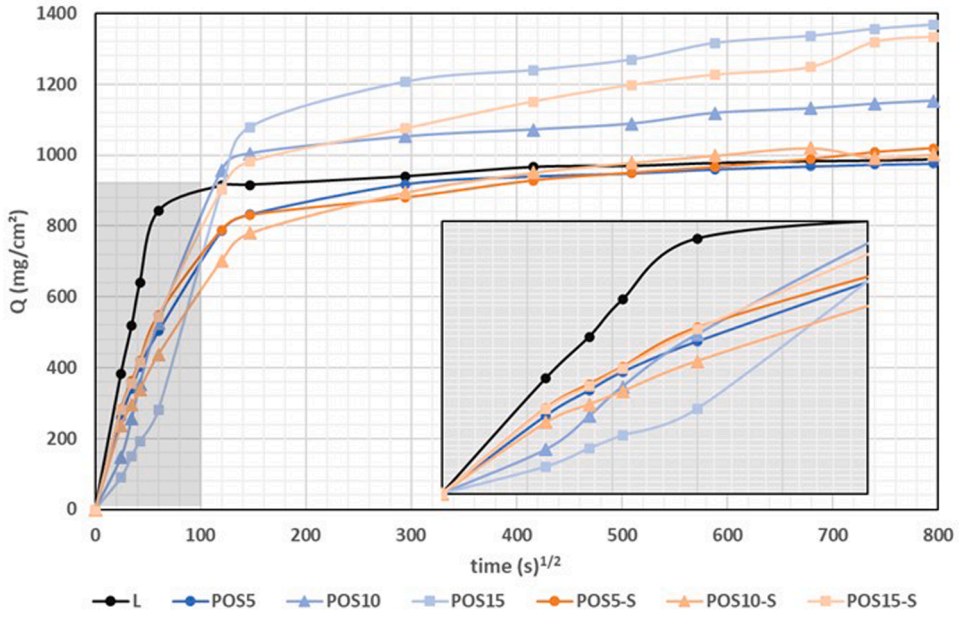

Fig. 2. Capillary absorption curves of reference and experimental mortars specimens.

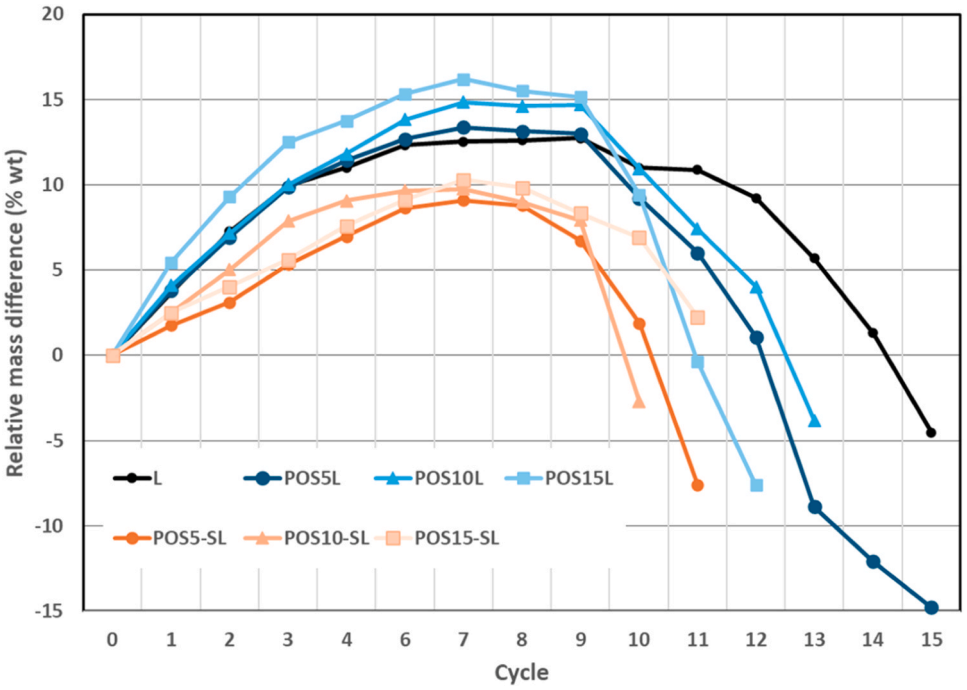

Fig. 3. Curve representing the weight variation of olive-stone and reference mortars during the salt crystallization cycles.

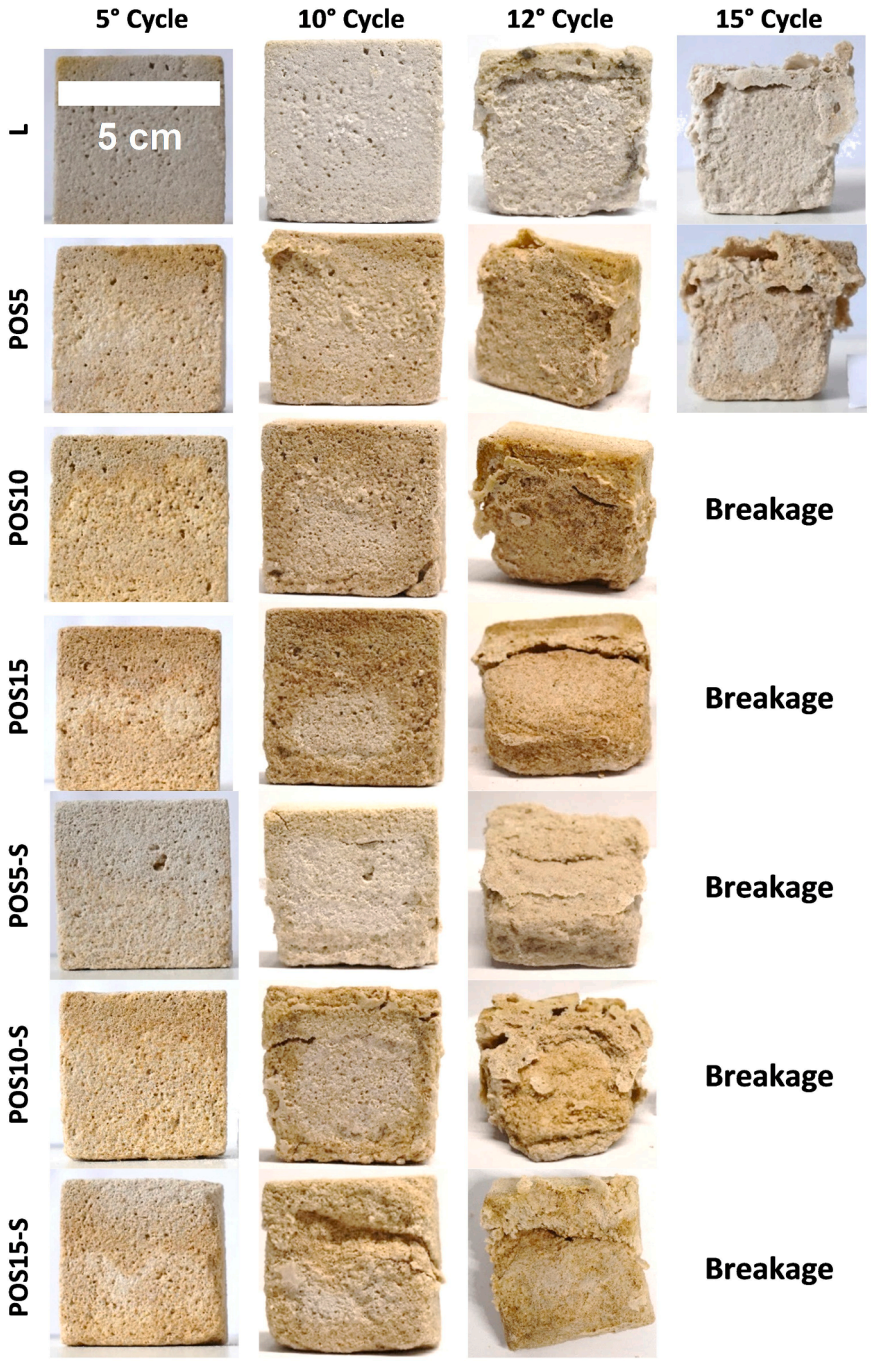

Fig. 4. Salt weathering developed in the formulated mortars during the test cycles.

no longer enough to counteract the mass lost. As a result, both POSL and POS-SL specimens began to experience severe mass loss accompanied by diffused macroscopic exfoliation and cracking phenomena (Fig. 4).

Notably, POS5L underwent a sharp mass reduction to −15 % by the fifteenth cycle, while the POS10L and POS15L mortars exhibited breakage during the fourteen and thirteen cycles, respectively.

Although POS-SL mortars showed less mass increase during the initial cycles, they exhibited more rapid degradation than the POSL mortars, with none of the nano silica specimens surviving beyond the eleventh cycle due to disintegration. As for the L specimens, despite undergoing considerable damage throughout the test, they remained physically cohesive until the end of the fifteen cycles, with a final mass loss of −5 %.

Overall, POS-modified mortars exhibited the highest initial mass gain due to increased porosity, particularly POS15L, which experienced the most significant uptake. This high salt absorption led to an accelerated degradation, with POS15L disintegrating by the 13th cycle. These findings indicate that a high POS content enhances salt ingress and crystallization, still leading to structural weaknesses.

Mortars modified with nano silica (POS-SL series) demonstrated improved early-stage performance, characterized by lower initial mass gain and reduced salt accumulation, likely due to a dense porous network created by the nanosilica addition. Nevertheless, these mortars underwent more severe degradation compared to their POS-only counterparts, with POS10-SL and POS5-SL mortars failing by the 12th cycle. Although nano silica initially enhances resistance by densifying the microstructure, it may exacerbate internal stresses due to salt crystallization in finer pores, leading to premature failure. Indeed, it is well

known that capillary pressure is inversely proportional to the network pore radius [45].

When comparing both mortar types, although POSL mortars absorbed more salt, they showed a slightly higher durability with respect to the POS-SL ones. On the contrary, nano silica-modified mortars delayed deterioration but failed abruptly. Ultimately, the reference mortars showed the highest durability, surviving all test cycles.

3.3. Mechanical performance and SEM and OM observations

The results of the bulk density measurements are presented in Fig. 5. In general, the bulk density values of the reference mortars are higher compared to those of the POSL and POS-SL formulations. Specifically, mortars prepared with lime and siliceous aggregate alone exhibited average bulk density values of approximately 1.64 g/cm^3 , which aligns with previously reported values for similar formulations [46]. The incorporation of POS led to a significant decrease in bulk density, particularly at higher replacement levels. Average bulk density values dropped from 1.51 g/cm^3 (POS5) to 1.38 g/cm^3 (POS15), a reduction that can be attributed to the lower intrinsic density of the olive stone powder compared to siliceous sand [47,48]. Conversely, the addition of nanosilica resulted in a partial recovery of bulk density values, with POS5-SL mortars reaching an average of 1.58 g/cm^3 . This trend is likely due to the formation of a denser matrix promoted by the presence of silica nanoparticles, which react with calcium hydroxide to form calcium silicate hydrate (C–S–H) phases [49].

This hypothesis is supported by the results obtained from the SEM-EDS investigation. In particular, SEM analysis enabled the observation of the L mortars matrix and the morphology of olive stone particles embedded within the POS15L and POS15-SL mixtures. The back-scattered electron images (BSE) are reported in Fig. 6. The olive stone powder particles exhibited sizes ranging from approximately 370 μm to 80 μm and displayed a dense, rough surface texture. They appeared as bundles of cells characterized by large lumens and cracks, as illustrated in Fig. 6 B,C [50,51].

EDS analyses performed on the POS15L sample provided the chemical characterization of the olive stone particles. The results confirmed the expected dominance of carbon (49.75 wt%) and oxygen (40.91 wt %), accompanied by minor amounts of calcium (4.84 wt%) and silicon (2.26 wt%), and traces of sodium (0.70 wt%) and potassium (0.88 wt %). These findings are consistent with those reported in recent literature [52].

In addition, spot microanalyses were conducted on homogeneous areas within the binder matrix of all mortar samples. In the L and POS15L samples, the results mainly showed high concentrations of CaO and MgO (from 87 to 97 wt%), reflecting the carbonate nature of the lime binder, along with lower SiO_2 contents (ranging from 2 to 10 wt%), attributable to the presence of finely dispersed siliceous aggregate.

A systematic and substantial increase in SiO_2 content (up to 16 wt%) was observed in the binder matrix of the POS15-SL sample, indicating the occurrence of pozzolanic reactions between the nanosilica released from the olive stone powder and the lime binder. Moreover, in this sample, microchemical analyses performed at the interface between the binder and the nanosilica-impregnated olive stone showed an average composition of 20.15 wt% SiO_2, 67.437 wt% CaO, 3.418 wt% Na_2O, 3.406 wt% MgO, and 4.239 wt% K_2O, suggesting the C-S-H phases formation.

In addition, the mechanical performance of the experimental mortars was assessed. The results of flexural and compressive strength are illustrated in Fig. 7A,B. This test is critical in the design of repair mortars in verifying their ability to provide sufficient strength to support structural loads and maintain the durability and integrity of the repaired sections. It also assesses the compatibility of the repair mortars with the original materials in the heritage structure, as mismatched mechanical properties could lead to differential stresses, cracking, and compromised structural stability [53].

Data showed that the reference sample (L), made of 100 % quartz aggregates, consistently exhibited the highest flexural and compressive strengths, with average values of 1 MPa and 1.52 MPa respectively. The inclusion of POS led to a reduction in strength as the POS content increased, with the highest performance observed in POS5L, which closely matched the reference sample. The decline in flexural and compressive strength was more pronounced in samples with higher POS content, such as POS10L and POS15L, possibly due to the increased porosity introduced by the POS.

Meanwhile, mortars with the addition of nano silica (POS-SL series) showed even further reductions in flexural and compressive strength compared to the POSL specimens, suggesting that nano silica may negatively impact tensile properties when combined with POS.

UPV measurements are in line with the results of the flexural and compressive strength (Fig. 8).

The reference specimens (L) showed the highest UPV values (2014.69 m/s). This indicates the densest structure and best mechanical integrity, likely due to the pure quartz powder and lime combination without replacements. UPV decreases as the percentage of olive stone replacement increases (POS5: 1897.98 m/s, POS10: 1710.14 m/s, POS15: 1630.80 m/s), because POS is less dense and introduces porosity, reducing material compactness. Adding nano silica further reduces UPV (POS5-S: 1611.05 m/s, POS10-S: 1588.74 m/s, POS15-S: 1370.63 m/s) which could be attributed to changes in the stress distribution within the mortar matrix.

In a review by Altawaiha et al., it was opined that even though adding nano-silica to concrete mixtures decreases porosity and enhances its pozzolanic interaction with calcium hydroxide, leading to the production of CSH and improved mechanical performance, researchers however caution the against the use of excessive amounts of nano-silica,

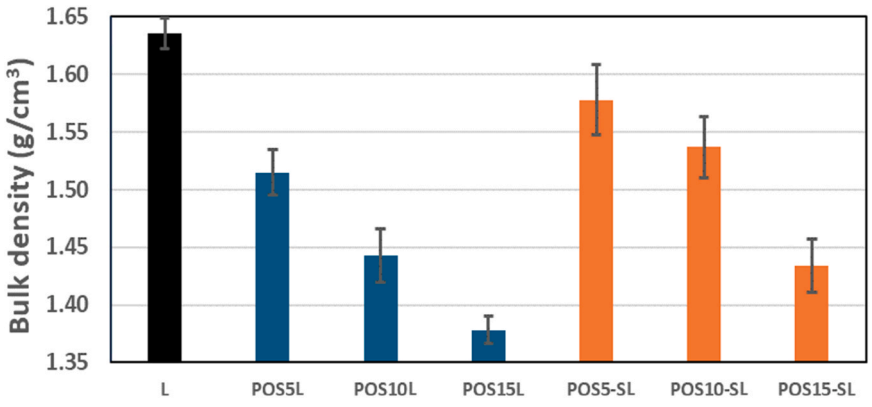

Fig. 5. Bulk density values of olive-stone and reference mortars.

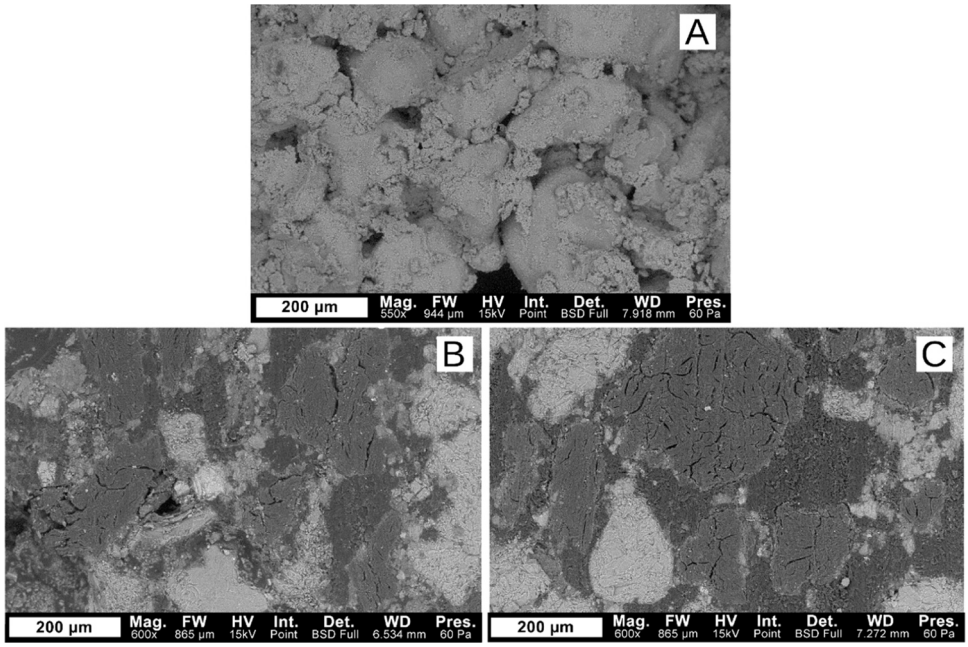

Fig. 6. SEM-BSE images of the reference L (A), POS15L (B) and POS15-SL (C) mortar matrix.

as it may cause particle aggregation within the cement matrix, weakening the bonds in its internal structure [54]. However, the reduction in mechanical strength observed in this study cannot be attributed to an excessive use of nano-silica. Another research [55], emphasized that the strength of concrete is primarily influenced by the strength of its aggregates, the cement matrix, and the interfacial transition zone (ITZ) between them. Their research revealed that, after 28 days of curing, mortar mixes incorporating recycled aggregates and silica fume demonstrated a significant reduction in compressive strength compared to natural aggregate concrete. They attributed this short-term reduction to the presence of cracks and impurities in the recycled aggregates, which hinder the effectiveness of silica fume as these impurities weaken the bond between the cement matrix and the aggregates, thereby diminishing the pozzolanic and filler effects of silica fume.

In line with these findings, POS, likely introduces inherent porosity, into the mortar matrix. This characteristic disrupts the bond between the aggregates and the cementitious matrix, potentially weakening the overall structure.

Although nano silica is known for its pozzolanic and filler effects, which reduce porosity and improve the bond between the binder matrix and aggregates, its effectiveness in this case may have been limited by these structural deficiencies introduced by the POS aggregates in this case, whose porous nature could have contributed to a weaker interfacial transition zone (ITZ) between the aggregates and the binder matrix, diminishing the ability of nano silica to effectively strengthen the structure. Furthermore, these flaws can act as stress concentration points, reducing both flexural and compressive strength, aligning with the research findings of Dilbas et al. [55].

Additionally, if nano silica is not uniformly distributed within the matrix, particle aggregation may occur, further weakening the internal bonds and contributing to the reduction in mechanical strength [56]. It is well known that the uneven distribution of nano silica within the matrix can lead to particle aggregation, weakening internal bonds and reducing mechanical strength [56].

To verify this hypothesis, image analysis was carried out on nine OM acquisitions of the POS15L and POS15-SL samples to determine the POS particle size distribution within the mortar mixtures. Following acquisition, the images were pre-processed to isolate POS particles from the surrounding mortar matrix. The processed images were then analysed using the ImageJ software. Each micrograph was converted into an 8-bit format and subsequently subjected to a segmentation procedure to extract quantitative information on the particles. Finally, data regarding the particle area were obtained (Fig. 9).

The quantitative analysis of particle areas reveals a pronounced concentration of POS particles in the smallest size class for both mortar types. Specifically, about 97 % of POS15L particles and about 95 % of POS15-SL particles fall within the first bin (0.008 and 2.1891 mm^2), indicating a dominant presence of fine grains. However, while POS15L displays a narrow and uniform distribution with no particles detected beyond 10.91 mm^2, POS15-SL exhibits a slightly broader particle size range, with small percentages extending up to 21.82 mm^2. These larger area values in POS15-SL may reflect the occurrence of larger clusters due to particle agglomerates.

Moreover, a Wilcoxon test was conducted to compare the area distributions of POS15L and POS15-SL particles (H_0, null hypothesis = particle distributions of each sample come from the same population). The results showed that the median particle area was significantly lower in POS15 (Mdn = 0.05 mm^2) compared to POS15-SL (Mdn = 0.11 mm^2). The test indicated a statistically significant difference between the two groups ($W = 0$, $p < .001$). Since the p value is below the 0.05 significance threshold, the null hypothesis that the two samples originate from the same population, was rejected. These findings suggest that POS15L and POS15-SL have significantly different particle area distributions, with POS15-SL containing a higher proportion of larger particles, likely due to increased aggregation, giving as result the reduction of mechanical performance.

4. Conclusions

This study investigated the use of Powdered Olive Stone (POS) as a sustainable partial replacement for quartz in lime-based mortars, assessing the effects of POS content (5–15 %) and nano-silica addition on their physical and mechanical properties.

A range of measurements, tests, and analytical investigations were conducted for this purpose, including colorimetric measurements, water absorption by capillarity tests, bulk density determinations, UPV measurements and compressive and flexural strength tests, as well as OM and SEM-EDS analyses. Furthermore, durability was assessed through salt crystallization tests.

The main results can be summarized as follows:

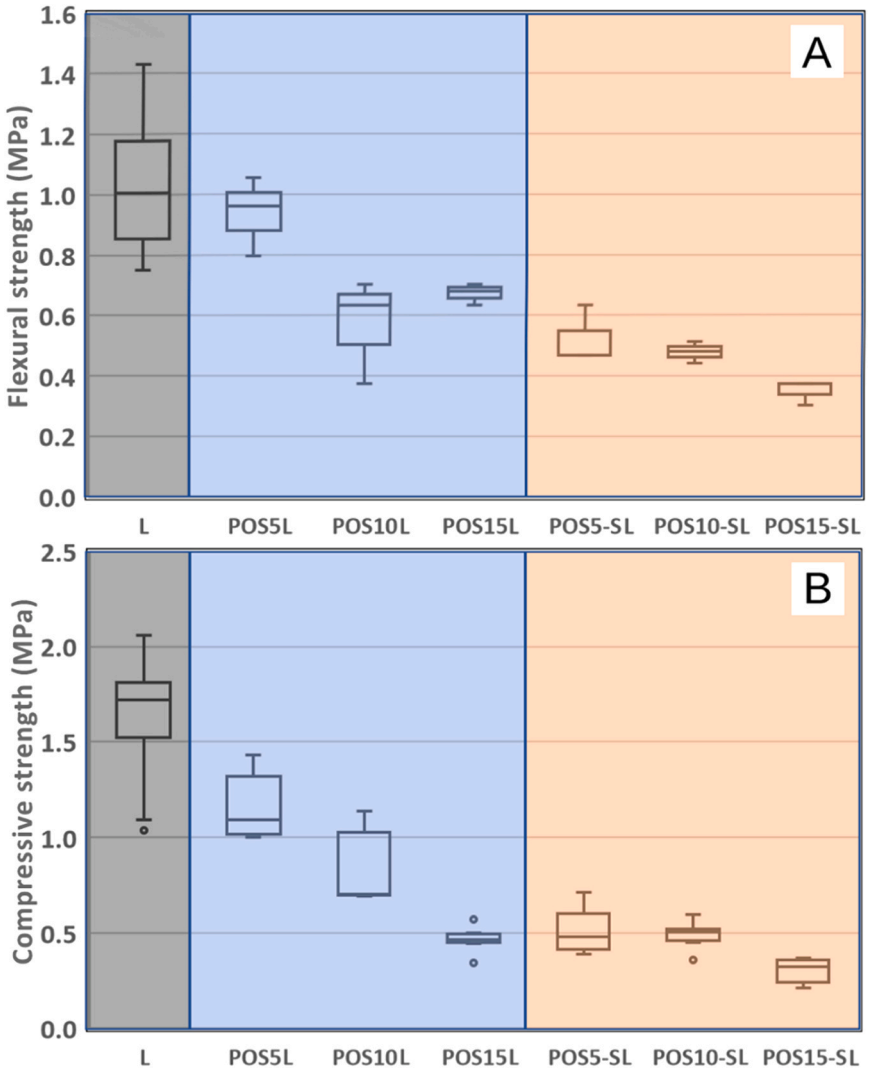

Fig. 7. Flexural and compressive strength of reference and POS mortars specimens.

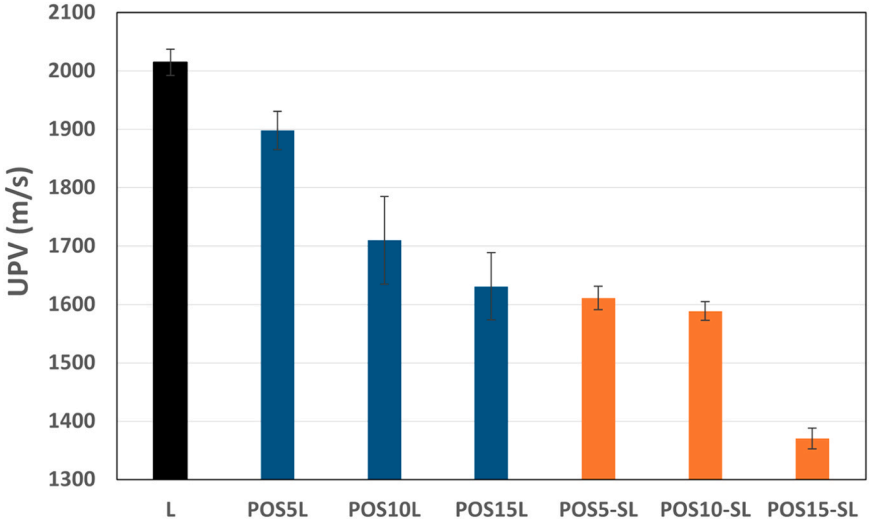

Fig. 8. Ultrasonic pulse velocity test and values of the reference and POSL and POS-SL mortars specimens.

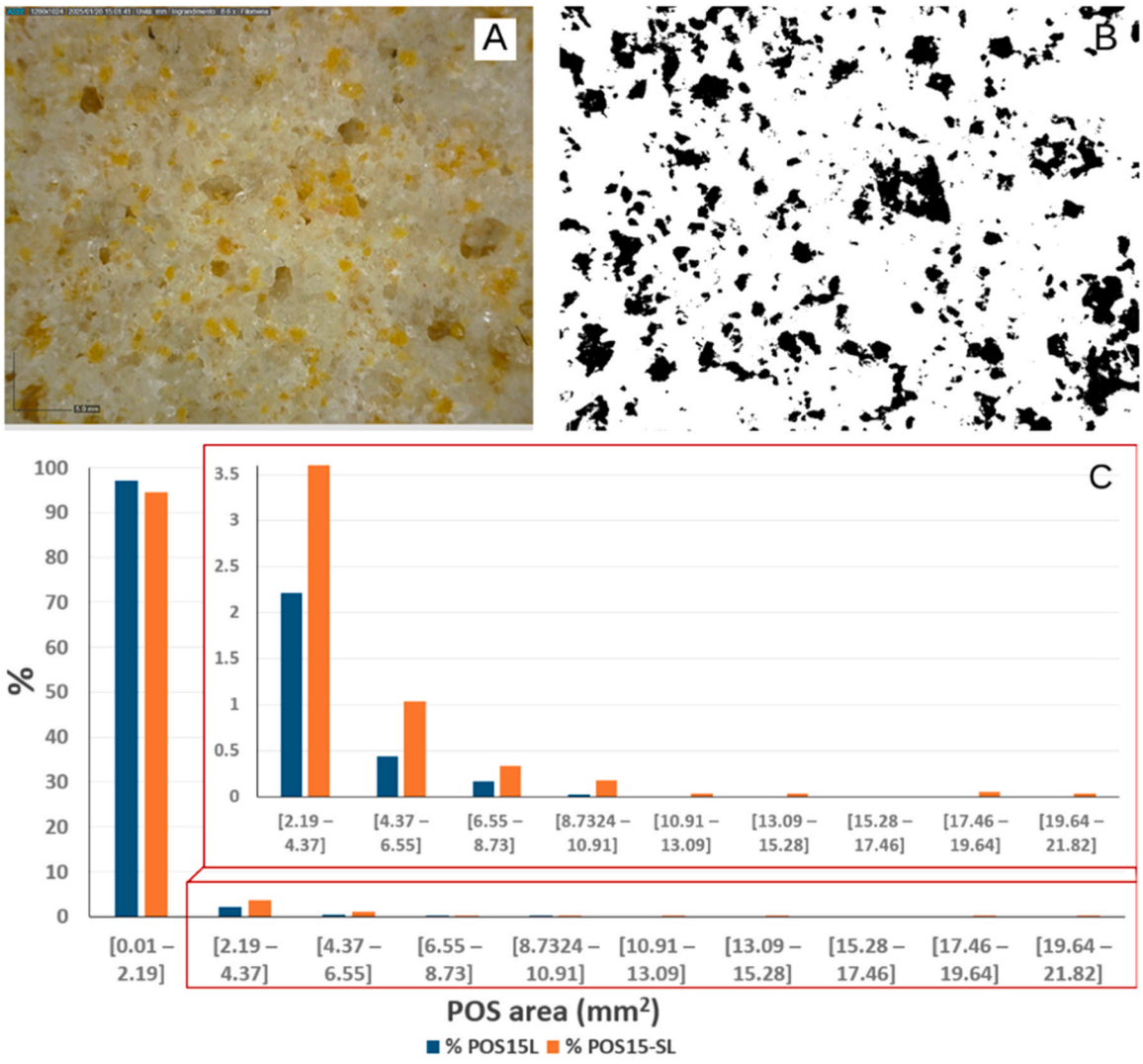

Fig. 9. (A) Micrograph of sample POS15-S showing the distribution of POS particles within the mortar matrix. (B) Image obtained through thresholding processing and segmentation, highlighting POS particles (in black) isolated from the matrix. (C) Histogram of the distribution of POS particle areas for samples POS15 and POS15-S. The x-axis represents particle area ranges (in mm^2), while the y-axis shows the percentage of total particles in each bin.

- Increasing POS content darkened the mortars and shifted their hue toward red and yellow, due to the natural colour of POS. Nano-silica mitigated these changes at low POS substitution, but its effect decreased at 15 % POS, with all variations remaining acceptable for aesthetic purposes.
- POS increased mortar porosity and water absorption, potentially acting as a sacrificial material to protect historical surfaces from crystallization damage.
- The addition of nano-silica reduced water uptake by densifying the pore network, enhancing early resistance to salt crystallization, but causing more severe long-term degradation compared to POS-only mortars.
- POS reduced bulk density, UPV, and mechanical strength due to its porous, low-density nature; nano-silica partially restores density but does not improve mechanical performance.
- POS-SL mortars show lower flexural and compressive strength, likely due to a weakened interfacial transition zone (ITZ) and particle agglomeration, as confirmed by optical microscopy.

Overall, this research indicates that the careful formulation and optimization of POS-containing mortars are crucial for meeting the specific requirements of conservation projects, paving the way for future exploration into the long-term performance of these materials in real-world conditions.

Funding sources

This research is funded by PNRR, TECH4YOU - "Technologies for Climate Change Adaptation and Quality of Life Improvement", CUP H23C22000370006, Project Code: ECS_00000009.

CRediT authorship contribution statement

Mauro Francesco La Russa: Writing – original draft, Project administration, Funding acquisition. **Andrea Macchia:** Validation, Investigation, Conceptualization. **Francesca Giordano:** Validation, Investigation. **Nicola Schiavon:** Writing – review & editing, Supervision, Project administration. **Silvestro Antonio Ruffolo:** Writing – review & editing, Writing – original draft, Validation, Supervision, Methodology, Investigation, Formal analysis, Data curation, Conceptualization. **Regina Adomako:** Writing – original draft, Validation, Investigation, Formal analysis, Data curation. **Maria Antonietta Zicarelli:** Writing – review & editing, Writing – original draft, Methodology, Investigation, Formal analysis, Data curation.

Declaration of Competing Interest

The authors declare that they have no known competing financial interests or personal relationships that could have appeared to influence the work reported in this paper.

Data availability

Data will be made available on request.

References

[1] U.J. Alengaram, B.A.A. Muhit, Utilization of oil palm kernel shell as lightweight aggregate in concrete – a review, Constr. Build. Mater. 38 (2013) 161–172, https://doi.org/10.1016/j.conbuildmat.2012.08.026.

[2] A.A. Firoozi, A.A. Firoozi, D.O. Oyejobi, S. Avudaiappan, E.S. Flores, Emerging trends in sustainable building materials: technological innovations, enhanced performance, and future directions, Results Eng. 24 (2024) 103521, https://doi.org/10.1016/j.rineng.2024.103521.

[3] A.S. Ruviaro, G.T. dos Santos Lima, L. Silvestro, M.T. Barraza, J.C. Rocha, J. de Brito, P.J.P. Gleize, F. Pelisser, Characterization and investigation of the use of oat husk ash as supplementary cementitious material as partial replacement of portland cement: analysis of fresh and hardened properties and environmental assessment, Constr. Build. Mater. 363 (2023) 129762, https://doi.org/10.1016/j.conbuildmat.2022.129762.

[4] W.T. Xu, T.Y. Lo, S.A. Memon, Microstructure and reactivity of rich husk ash, Constr. Build. Mater. 29 (4) (2012) 541–547, https://doi.org/10.1016/j.conbuildmat.2011.11.005.

[5] Y. Abubakar, M.U. Attah, U. Muazu, An assessment of pozzolanic properties of wheat husk ash (WHA), Int. Res. J. Adv. Eng. Sci. 7 (2) (2022) 73–76.

[6] S. Blesson, A.U. Rao, Agro-industrial-based wastes as supplementary cementitious or alkali-activated binder material: a comprehensive review, Innov. Infrastruct. Solut. 8 (4) (2023) 125, https://doi.org/10.1007/s41062-023-01096-8.

[7] J. He, S. Kawasaki, V. Achal, The utilization of agricultural waste as agro-cement in concrete: a review, Sustainability 12 (17) (2020) 6971, https://doi.org/10.3390/su12176971.

[8] M. Amare, S. Swara, M. Haish, A.K. Pani, P. Saha, Performance of agro-wastes and chemical admixtures used in concrete: a review, Mater. Today Proc. (2023), https://doi.org/10.1016/j.matpr.2023.08.058.

[9] S. Barbhuiya, B.B. Das, D. Adak, A comprehensive review on integrating sustainable practices and circular economy principles in concrete industry, J. Environ. Manag. 370 (2024) 122702, https://doi.org/10.1016/j.jenvman.2024.122702.

[10] J. Ferreiro-Cabello, E. Fraile-Garcia, A. Pernia-Espinoza, F.J. Martinez-de-Pison, Strength performance of different mortars doped using olive stones as lightweight aggregate, Buildings 12 (2022) 1668, https://doi.org/10.3390/buildings12101668.

[11] J. Kanadasan, A.F.A. Fauzi, H.A. Razak, P. Selliah, V. Subramaniam, S. Yusoff, Feasibility studies of palm oil mill waste aggregates for the construction industry, Materials 8 (9) (2015) 6508–6530, https://doi.org/10.3390/ma8095319.

[12] I.G.M. Özkan, K. Aldemir, O. Alhasan, A. Benli, O.Y. Bayraktar, M.U. Yilmazoglu, G. Kaplan, Investigation on the sustainable use of different sizes of sawdust aggregates in eco-friendly foam concretes: physico-mechanical, thermal insulation and durability characteristics, Constr. Build. Mater. 438 (2024) 137100, https://doi.org/10.1016/j.conbuildmat.2024.137100.

[13] P. Kampragkou, M. Dabekaussen, V. Kamperidou, M. Stefanidou, Bio-additives in lime-based mortars: an investigation of the morphology performance, Constr. Build. Mater. 474 (2025) 141177, https://doi.org/10.1016/j.conbuildmat.2025.141177.

[14] M.F. Junaid, Zu Rehman, M. Kuruc, I. Medve, D. Bacinskas, J. Curpek, M. Cekon, N. Ijaz, W.S. Ansari, Lightweight concrete from a perspective of sustainable reuse of waste byproducts, Constr. Build. Mater. 319 (2022) 126061, https://doi.org/10.1016/j.conbuildmat.2021.126061.

[15] A. San Vicente-Navarro, M. Mendívil-Giro, J. Los Santos-Ortega, E. Fraile-García, J. Ferreiro-Cabello, Alternative use of the waste from ground olive stones in doping mortar bricks for sustainable Façades, Buildings 13 (12) (2023) 2992, https://doi.org/10.3390/buildings13122992.

[16] M. Khemakhem, M. Jaziri, Composites based on (ethylene–propylene) copolymer and olive solid waste: rheological thermal, mechanical, and morphological behaviors, Polym. Eng. Sci. 56 (2016) 27–35, https://doi.org/10.1002/pen.24188.

[17] F. Barreca, C.R. Fichera, Use of olive stone as an additive in cement lime mortar to improve thermal insulation, Energy Build. 62 (2013) 507–513, https://doi.org/10.1016/j.enbuild.2013.03.040.

[18] T. Cheboub, Y. Senhadji, H. Khelafi, G. Escadeillas, Investigation of the engineering properties of environmentally friendly self-compacting lightweight mortar containing olive kernel shells as aggregate, J. Clean. Prod. 249 (2020) 119406, https://doi.org/10.1016/j.jclepro.2019.119406.

[19] L. Rilem, Functional classification of lightweight concrete, Mater. Struct. 11 (1978) 281–283.

[20] N.M. Al-Akhras, M.Y. Abdulwahid, Utilisation of olive waste ash in mortar mixes, Struct. Concr. 11 (2010) 221–228, https://doi.org/10.1680/stco.2010.11.4.221.

[21] E. Ghafari, H. Costa, E. Júlio, A. Portugal, L. Duˆ Aes, The effect of nanosilica addition on flowability, strength and transport properties of ultra high performance concrete, Mater. Des. 59 (2014) 1–9, https://doi.org/10.1016/j.matdes.2014.02.051.

[22] Y. Qing, et al., Influence of nano-SiO2 addition on properties of hardened cement paste as compared with silica fume, Constr. Build. Mater. 21 (3) (2007) 539–545, https://doi.org/10.1016/j.conbuildmat.2005.09.001.

[23] F. Althoey, O. Zaid, R. Martínez-García, F. Alsharari, M. Ahmed, M.M. Arbili, Impact of nano-silica on the hydration, strength, durability, and microstructural properties of concrete: a state-of-the-art review, Case Stud. Constr. Mater. 18 (2023) e01997, https://doi.org/10.1016/j.cscm.2023.e01997.

[24] P.P. Abhilash, D.K. Nayak, B. Sangoju, R. Kumar, V. Kumar, Effect of nano-silica in concrete; a review, Constr. Build. Mater. 278 (2021) 122347, https://doi.org/10.1016/j.conbuildmat.2021.122347.

[25] K. Elert, C. Rodriguez-Navarro, E.S. Pardo, E. Hansen, O. Cazalla, Lime mortars for the conservation of historic buildings, Stud. Conserv 47 (2002) 62–75, https://doi.org/10.1179/sic.2002.47.1.62.

[26] EN 1015-3:2001, Methods of test for mortar for masonry - part 3: determination of consistence of fresh mortar (by flow table), Eur. Comm. Stand. (CEN) (2001).

[27] EN 15886:2010, Conservation of cultural property - test methods - colour measurement of surfaces, Eur. Comm. Stand. (CEN) (2010).

[28] EN 15801:2010, Conservation of cultural property - test methods - determination of water absorption by capillarity, Eur. Comm. Stand. (CEN) (2010).

[29] EN 12370:1999, Natural stone test methods - determination of resistance to salt crystallization, Eur. Comm. Stand. (CEN) (2001).

[30] D. Benavente, M.A. García del Cura, A. Bernabéu, S. Ordóñez, Quantification of salt weathering in porous stones using an experimental continuous partial immersion method, Eng. Geol. 59 (3-4) (2001) 313–325, https://doi.org/10.1016/S0013-7952(01)00020-5.

[31] M. Ricca, E. Le Pera, M. Licchelli, A. Macchia, M. Malagodi, L. Randazzo, N. Rovella, S.A. Ruffolo, M.L. Weththimuni, M.F. La Russa, The CRATI project: new insights on the consolidation of salt weathered stone and the case study of san domenico church in cosenza (South Calabria, Italy), Coatings 9 (2019) 330, https://doi.org/10.3390/coatings9050330.

[32] B. Lubelli, I. Rörig-Daalgard, A.M. Aguilar, et al., Recommendation of RILEM TC 271-ASC: new accelerated test procedure for the assessment of resistance of natural stone and fired-clay brick units against salt crystallization, Mater. Struct. 56 (2023) 101, https://doi.org/10.1617/s11527-023-02158-0.

[33] EN 1015-11:2019, Methods of test for mortar for masonry - part 11: determination of flexural and compressive strength of hardened mortar, Eur. Comm. Stand. (CEN) (2019).

[34] EN 14579:2005, Natural stone test methods - determination of sound speed propagation, Eur. Comm. Stand. (CEN) (2005).

[35] EN 772-13:2002, Methods of test for masonry units - part 13: determination of net and gross dry density of masonry units (except for natural stone), Eur. Comm. Stand. (CEN) (2002).

[36] T.J. Collins, ImageJ for microscopy, Biotechniques 43 (2007) 25–30, https://doi.org/10.2144/000112517.

[37] K. Van Balen, I. Papayianni, R. Van Hees, L. Binda, A. Waldum, Introduction to requirements for and functions and properties of repair mortars, Mater. Struct. /Mater. Et. Constr. 38 (282) (2005) 781–785, https://doi.org/10.1617/14319.

[38] M.Mar Barbero-Barrera, L.S. Gomez-Villalba, D. Ergenç, A. Sierra-Fernandez, R. Fort, Influence of curing conditions on the mechanical and hydric performance of air-lime mortars with nano-Ca(OH)2 and nano-SiO2 additions, Cem. Concr. Compos 132 (2022) 104631, https://doi.org/10.1016/j.cemconcomp.2022.104631.

[39] M. Thomson, J.-E. Lindqvist, J. Elsen, C.J.W.P. Groot, Characterisation of old mortars with respect to their repair, chapter 2.5 characterisation: porosity of mortars, RILEM publications, 2007.

[40] M. Arandigoyen, J.L.Pérez Bernal, M.A.Bello López, J.I. Alvarez, Lime-pastes with different kneading water: pore structure and capillary porosity, Appl. Surf. Sci. 252 (5) (2005) 1449–1459, https://doi.org/10.1016/j.apsusc.2005.02.145.

[41] N.S. Martys, C.F. Ferraris, Capillary transport in mortars and concrete, Cem. Concr. Res. 27 (5) (1997) 747–760, https://doi.org/10.1016/S0008-8846(97)00052-5.

[42] J.J. Hughes, Rilem TC 203-RHM: repair mortars for historic masonry, role Mortar Mason. Introd. Requir. Des. Repair Mortars Mater. Struct. /Mater. Et. Constr. 45 (2012) 1287–1294, https://doi.org/10.1617/s11527-012-9847-9.

[43] M.F. La Russa, S.A. Ruffolo, Mortars and plasters - how to characterize mortar and plaster degradation, Archaeol. Anthropol. Sci. 13 (2021), https://doi.org/10.1007/s12520-021-01405-1.

[44] M.A. Zicarelli, M.F. La Russa, M.F. Alberghina, S. Schiavone, R. Greca, P. Pogliani, M. Ricca, S.A. Ruffolo, A multianalytical investigation to preserve wall paintings: a case study in a hypogeum environment, Materials 16 (4) (2023) 1380, https://doi.org/10.3390/ma16041380.

[45] M.F. La Russa, S.A. Ruffolo, M.A. de Buergo, M. Ricca, C.M. Belfiore, A. Pezzino, G. M. Crisci, The behaviour of consolidated neapolitan yellow tuff against salt weathering, Bull. Eng. Geol. Environ. 76 (2017) 115–124, https://doi.org/10.1007/s10064-016-0874-6.

[46] S. Pavía, B. Toomey, Influence of the aggregate quality on the physical properties of natural feebly-hydraulic lime mortars, Mater. Struct. 41 (3) (2008) 559–569, https://doi.org/10.1617/s11527-007-9267-4.

[47] J. Mata-Sanchez, J.A. Perez-Jimenez, M.J. Díaz-Villanueva, A. Serrano, N. Núnez-Sanchez, F.J. Lopez-Gimenez, Development of olive stone quality system based on biofuel energetic parameters study, Renew. Energy 66 (2014) 251–256, https://doi.org/10.1016/j.renene.2013.12.009.

[48] M. Cuevas, M.L. Martínez-Cartas, L. Perez-Villarejo, L. Hernandez, J.F. García, Matín, S. Sanchez, Drying kinetics and effective water diffusivities in olive stone and olive-tree pruning, Renew. Energy 132 (2019) 911–920, https://doi.org/10.1016/j.renene.2018.08.053.
[49] J.M. Fernández, A. Duran, I. Navarro-Blasco, J. Lanas, R. Sirera, J.I. Alvarez, Influence of nanosilica and a polycarboxylate ether superplasticizer on the performance of lime mortars, Cem. Concr. Res. 43 (2013) 12–24, https://doi.org/10.1016/j.cemconres.2012.10.007.
[50] E. Marinova, J.M.A. van der Valk, S.M. Valamoti, J. Bretschneider, An experimental approach for tracing olive processing residues in the archaeobotanical record, with preliminary examples from tell tweini, Syria, Veg. Hist. Archaeobotany 20 (2011) 471–478, https://doi.org/10.1007/s00334-011-0298-y.
[51] A.L. Winton, K.B. Winton, The structure and composition of foods, in: A.L. Winton, K.B. Winton (Eds.), Cereals, Starch, Oil Seeds, Nuts, Oils, Forage Plants, 1, Chapman and Hall, London, 1932.
[52] M. Olmedo-Navarro, J.M. Pérez, N. Gutiérrez-Segura, B. Sánchez-Sevilla, Y. Soriano-Jerez, D.A. Alonso, M.C. Cerón, I. Fernández, High degree of silanization of olive wood shell stone and its use in polyester biocomposites, RSC Sustain 2 (2024) 1030–1039, https://doi.org/10.1039/d3su00475a.
[53] TC 203-RHM (Jan Erik Lindqvist), Rilem TC 203-RHM: repair mortars for historic masonry. Testing of hardened mortars, a process of questioning and interpreting, Mater. Struct. 42 (2009) 853–865, https://doi.org/10.1617/s11527-008-9455-x.
[54] H. AlTawaiha, F. Alhomaidat, T. Eljufout, A review of the effect of nano-silica on the mechanical and durability properties of cementitious composites, Infrastructures 8 (9) (2023), https://doi.org/10.3390/infrastructures8090132.
[55] H. Dilbas, M. Simsek, O. Çakır, An investigation on mechanical and physical properties of recycled aggregate concrete (RAC) with and without silica fume, Constr. Build. Mater. 61 (2014) 50–59, https://doi.org/10.1016/j.conbuildmat.2014.02.057.
[56] H. Li, M. Zhang, J. Ou, Flexural fatigue performance of concrete containing nano-particles for pavement, Int. J. Fatig 29 (2007) 1292–1301, https://doi.org/10.1016/j.ijfatigue.2006.10.004.